Chen *et al. Chin. J. Mech. Eng.* (2021) 34:29
https://doi.org/10.1186/s10033-021-00548-5

Chinese Journal of Mechanical Engineering

ORIGINAL ARTICLE

Open Access

Research and Test of Three-Pulley Noncircular Synchronous Pulley Transmission Mechanism with Minimum Slack

Jianneng Chen[1,2*], Xincheng Sun[1], Chuanyu Wu[1,2], Dadu Xiao[1] and Jun Ye[1]

Abstract

The noncircular synchronous belt drive mechanism has demonstrated certain achievements and has been used in special fields. Research regarding noncircular synchronous belt drive mechanisms has focused on optimization design and kinematic analysis in China, whereas two pulley noncircular synchronous belt transmissions have been developed overseas. However, owing to the noncircular characteristics of the belt pulley, the real-time variation in the belt length slack during the transmission of the noncircular synchronous belt is significant, resulting in high probabilities of skipping and vibration. In this study, a noncircular tensioning pulley is added to create a stable three-pulley noncircular synchronous belt driving mechanism and a good synchronous belt tensioning, with no skipping; hence, the non-uniform output characteristic of the driven pulley is consistent with the theoretical value. In the circular noncircular noncircular three-pulley noncircular synchronous belt mechanism, the pitch curve of the driving synchronous belt pulley is circular, whereas those of the driven synchronous belt and tensioning pulleys are noncircular. To minimize the slack of the belt length of the synchronous belt and the constraint of the concavity and circumference of the tensioning pulley, an automatic optimization model of the tensioning pulley pitch curve is established. The motion simulation, analysis, and optimization code for a three-belt-pulley noncircular synchronous belt drive mechanism is written, and the variation in belt length slack under different speed ratios is analyzed based on several examples. The testbed for a circular–noncircular–noncircular three-pulley noncircular synchronous belt transmission mechanism is developed. The test shows that the three-pulley noncircular synchronous belt drives well. This study proposes an automatic optimization algorithm for the tensioning pulley pitch curve of a noncircular synchronous belt transmission mechanism; it yields a stable transmission of the noncircular synchronous belt transmission mechanism as well as non-uniform output characteristics.

Keywords: Noncircular synchronous belt drive, Slack calculation model, Non-uniform speed transmission characteristics

1 Introduction

During one rotation period of a noncircular synchronous belt transmission mechanism, the required theoretical belt length changes in real time owing to the real-time changes of the noncircular synchronous belt pulley diameters in a transmission cycle. The amount of slack is the difference between the maximum and minimum values of the required belt length. An excessive amount of slack can cause tooth skipping, rendering it impossible to achieve accurate non-uniform output characteristics.

Satchel [1] and Wu et al. [2, 3] presented models for calculating the noncircular belt pulley pitch curve required for the transmission ratio based on different methods, but no discussion regarding tensioning was provided. Konishi et al. [4] and Guo et al. [5] used eccentric circular gears to design a rice transplanting mechanism that can satisfy the specific motion of planting.

*Correspondence: jiannengchen@zstu.edu.cn
[1] Faculty of Mechanical Engineering and Automation, Zhejiang Sci-Tech University, Hangzhou 310018, China
Full list of author information is available at the end of the article

Liu et al. [6], Ottaviano et al. [7], and Li [8] investigated many types of noncircular gears, such as elliptical gears, eccentric circular gears, noncircular helical gears, and gears with lobes. Finally, eccentric circular gears were used to design a rice transplanting mechanism that can satisfy the specific motion of planting. Karpov et al. [9] and Freudenstein et al. [10] proposed a method to calculate slack in the noncircular two-pulley synchronous belt transmission process. It was discovered that the two-pulley synchronous belt transmission could not maintain real-time tension during a drive cycle. Zheng et al. [11] used a noncircular belt drive on a punching machine to obtain better quick-return characteristics, satisfying the requirements of a slow operating speed. However, only two noncircular pulleys were discussed. The calculation showed that the amount of slack changed during a drive cycle, and the maximum slack was 114.4 mm. Feng et al. [12] attempted to obtain the minimum theoretical slack of the belt (chain) length when the center distance was 100 mm, and the transmission law involved the driving and driven pulley angles. The parameters of the eccentric circle belt (chain) pulley mechanism were optimized. When the eccentricity was 0.16, a minimum theoretical slack of 2.62 mm was obtained without considering the polygon effect. Yang et al. [13] established a three-pulley noncircular synchronous belt transmission model and regarded the driving pulley as a circle. Using an objective function with the smallest change in the theoretical belt length at any time during the rotation period, the objective function was optimized to obtain a set of optimal parameters. After the optimization was performed, the variance of the length change of the band was 46.91 in one cycle. Cao et al. [14] established a continuous mapping model of two-belt (chain) pulley transmissions, and the speed ratio function was calculated while considering the polygon effect, and the law of belt (chain) transmission was obtained.

In summary, whether it is a two-pulley noncircular synchronous belt drive without a tensioner or a three-pulley noncircular synchronous belt drive with a noncircular tensioner, the slack of the belt length is large when a slight change occurs in the transmission ratio. Furthermore, the amount of slack will not cause real-time tensioning or skipping in the synchronous belt drive, thereby nullifying the predetermined precise non-uniform speed transmission rule.

The uneven variation in the belt length slack during a noncircular synchronous belt transmission renders it difficult to achieve accurate non-uniform speed transmission in engineering applications. He [15] proposed a circular–eccentric circular–noncircular belt pulley drive mechanism, in which the noncircular belt pulley was the tensioning pulley and the belt length slack was the objective function. The slack value was 10.36 mm when the center distance of the belt pulley was 110 mm after manual optimization. The method involved fitting and backward generation, which necessitated a significant amount of calculation; hence, the results obtained were low in precision.

Following the results of He [15], the author studied the variation in slack in a three-pulley noncircular synchronous belt transmission with a noncircular tensioning pulley, analyzed the characteristics of the three-pulley noncircular synchronous belt transmission, and conducted experimental research.

2 Three-Pulley Noncircular Synchronous Belt Drive Belt Length Calculation Model

As shown in Figure 1, a circular–noncircular three-pulley noncircular synchronous belt transmission mechanism that included driving pulley 1 with a circular pitch curve, driven pulley 2 with a noncircular pitch curve, and tension pulley 3 with a noncircular pitch curve was considered. The circumferences of the three pulleys were identical. The pitch curve of synchronous pulley 2 was determined based on the transmission relationship between the driving and driven pulleys, and the pitch curve of the synchronous belt tension pulley 3 was determined based on the theoretical optimization of the minimum slack of the synchronous belt in the transmission.

2.1 Tangent Polar Coordinate Equation of Plane Curve

The plane coordinate system *o-xy* comprised an arbitrary curve *c*. As shown in Figure 2, the tangent at point $C(x, y)$ on the curve is *t*, *ON* is the vertical distance from the origin

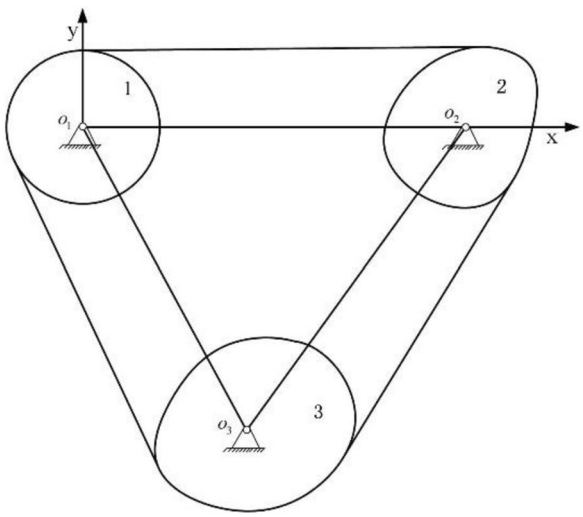

Figure 1 Schematic of three-pulley noncircular synchronous belt transmission mechanism

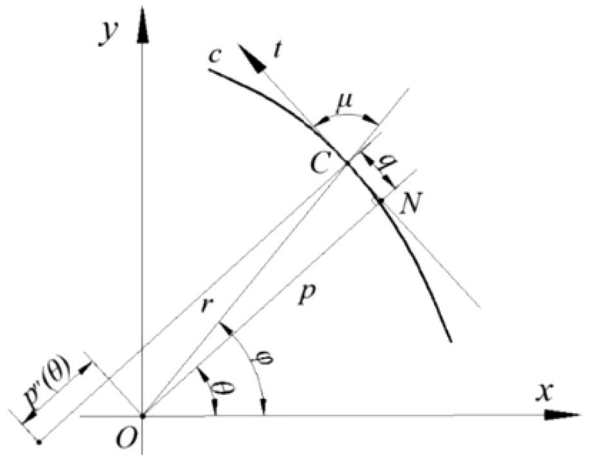

Figure 2 Curve and tangent in polar coordinates

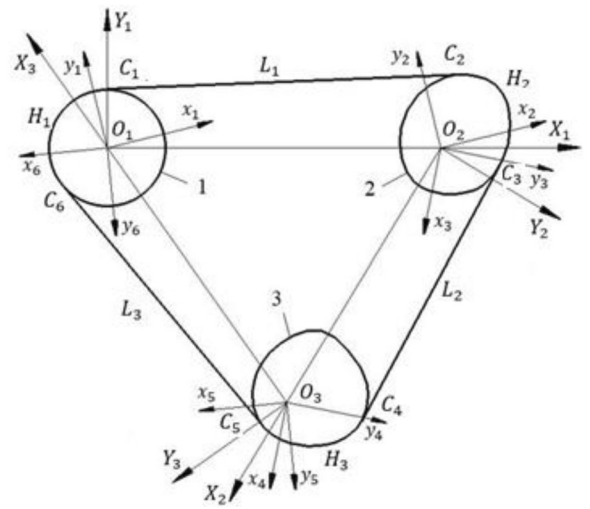

Figure 3 Schematic diagram of coordinate system of noncircular three-pulley synchronous belt transmission mechanism and calculation of belt length: 1. Driving pulley, 2. Driven pulley, 3. Tension pulley

O to the tangent t, the foot point is N, the vertical distance ON recorded is denoted as p (hereinafter referred to as the tangential diameter), the length of the line segment CN is denoted as q, and the length of vector OC is denoted as r. The angle between the ox-axis and vector OC is ϕ, and the angle between the ox-axis and the perpendicular ON is θ, (hereinafter referred to as the tangential angle). Hence, the tangent polar coordinate equation of the curve is [16, 17]

$$p(\theta) = x\cos\theta + y\sin\theta. \tag{1}$$

Based on Eq. (1), the first derivative of p with respect to θ is expressed as

$$-x\sin\theta + y\cos\theta = p'(\theta). \tag{2}$$

Based on the geometric relationship shown in Figure 2 [18], we obtain

$$q = CN = r\cos u, \tag{3}$$

$$CN = p'(\theta). \tag{4}$$

Solving Eqs. (1) and (2), the relationship between the Cartesian coordinates of curve c and the tangent polar coordinates is as follows:

$$\begin{cases} x = p(\theta)\cos\theta - p'(\theta)\sin\theta, \\ y = p(\theta)\sin\theta + p'(\theta)\cos\theta. \end{cases} \tag{5}$$

2.2 Pitch Curve Calculation Model of Synchronous Belt Pulley in Three-Pulley Noncircular Synchronous Belt Drive

As shown in Figure 3, the rotation centers of driving pulley 1, driven pulley 2, and tension pulley 3 are denoted as O_1, O_2, and O_3, respectively. We define O_1-XY as the fixed reference frame; and $o_1 - x_1y_1$, $o_2 - x_2y_2$, and $o_3 - x_3y_3$ as the moving reference frames attached to pulleys 1, 2, and 3, respectively. The center distance between the two pulleys is $o_1o_2 = a$, the transmission ratio between the driving and driven pulleys is i_{12}, and the initial rotation angle of driving pulley 1 and driven pulley 2 is $\varphi_1 = \varphi_2 = 0$. The driving pulley rotates counterclockwise, and the rotation angle between the driving and driven pulley exhibits the following relationship:

$$\varphi_2 = \int_0^{\varphi_1} \frac{1}{i_{12}} \mathrm{d}\varphi_1. \tag{6}$$

Figure 4 shows that, in moving coordinate system $o_1 - x_1y_1$, the angle between axis x_1 and the tangential diameter p_1 of the driving pulley is θ_1. In moving coordinate system $o_2 - x_2y_2$, the angle between axis x_2 and the

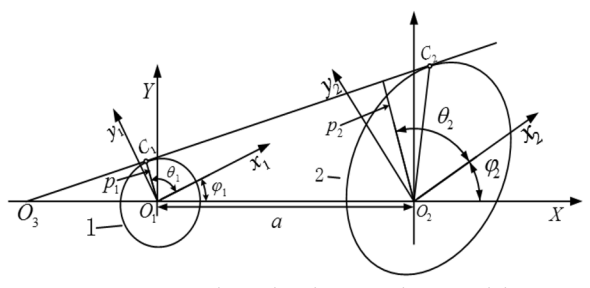

Figure 4 Transmission relationships between driving and driven pulleys

tangential diameter p_2 of the driving pulley is θ_2. The relationship between the tangential and rotation angles can be written as

$$\theta_1 = \theta_2 + \varphi_2 - \varphi_1. \tag{7}$$

The driving pulley pitch curve is a circle with a fixed radius, and the tangential polar coordinate equation is expressed as follows:

$$p_1 = p_1(\theta_1). \tag{8}$$

Based on the relationships shown in Figure 4, Eqs. (7) and (8) yield the following:

$$\cos(\theta_1 + \varphi_1) = -\frac{p_1(\theta_1) \times (i_{12} - 1)}{a}. \tag{9}$$

Based on Eqs. (5) and (8), the rectangular coordinates of the pitch curve of the driving pulley in coordinate system $o_1 - x_1y_1$ are expressed as follows:

$$\begin{cases} x_1 = p_1(\theta_1)\cos(\theta_1) - p_1^{'}(\theta_1)\sin(\theta_1), \\ y_1 = p_1(\theta_1)\sin(\theta_1) + p_1^{'}(\theta_1)\cos(\theta_1). \end{cases} \tag{10}$$

According to tangent polar coordinate theory, the relationship between the driving and driven pulley tangential diameters is expressed as

$$p_2 = p_1 \times i_{12}. \tag{11}$$

For a rotation angle ϕ_1, Eqs. (8) and (9) can be solved to obtain p_1 and θ_1, whereas Eqs. (6), (7), and (10) can be solved to obtain p_2 and θ_2. Hence, we obtain a tangent polar coordinate equation for the driven pulley curve as follows:

$$p_2 = p_2(\theta_2). \tag{12}$$

Based on Eqs. (5) and (12), the driving pulley rotation angle is ϕ_1, and the driven pulley rotation angle is ϕ_2. Moving coordinate system $o_2 - x_2y_2$ can be expressed in rectangular coordinates as follows:

$$\begin{cases} x_2 = p_2(\theta_2)\cos(\theta_2) - p_2^{'}(\theta_2)\sin(\theta_2), \\ y_2 = p_2(\theta_2)\sin(\theta_2) + p_2^{'}(\theta_2)\cos(\theta_2). \end{cases} \tag{13}$$

The initial tension pulley pitch curve is a circle of radius the same as that of the driving pulley. The driving and tension pulley rotation angles are denoted as ϕ_1 and ϕ_3, respectively. Hence, the tangent polar coordinate equation of the tension pulley pitch curve is as follows:

$$p_3 = p_3(\theta_3). \tag{14}$$

Based on Eqs. (5) and (14), moving coordinate system $o_3 - x_3y_3$ can be expressed in rectangular coordinates as follows:

$$\begin{cases} x_3 = p_3(\theta_3)\cos(\theta_3) - p_3^{'}(\theta_3)\sin(\theta_3), \\ y_3 = p_3(\theta_3)\sin(\theta_3) + p_3^{'}(\theta_3)\cos(\theta_3). \end{cases} \tag{15}$$

2.3 Three-Pulley Noncircular Synchronous Belt Drive Belt Length Calculation Model

The driving, driven, and tension pulleys rotate by φ_1, φ_2, and ϕ_3, respectively. The tangent points between the synchronous belt and driving pulley 1 and the between driven pulley 2 and tension pulley 3 are shown in Figure 3. The tangent polar coordinate parameters of tangent points C_1, C_2, C_3, C_4,C_5, andC_6 are p_1 and θ_{12}, p_2 and θ_{21}, p_2 and θ_{23}, p_3 and θ_{34}, p_3 and θ_{35}, and p_1 and θ_{16}, respectively. The total belt length of the noncircular three-pulley synchronous belt transmission mechanism can be written as

$$S = \overline{C_1C_2} + \overset{\frown}{C_2C_3} + \overline{C_3C_4} + \overset{\frown}{C_4C_5} + \overline{C_5C_6} + \overset{\frown}{C_6C_1}. \tag{16}$$

In Eq. (16), $\overline{C_1C_2}$, $\overline{C_3C_4}$, and $\overline{C_5C_6}$ are the lengths of the common tangents between the two pulleys, and $\overset{\frown}{C_2C_3}$, $\overset{\frown}{C_4C_5}$, and $\overset{\frown}{C_6C_1}$ are the arc lengths corresponding to the wrapping angles formed between the two tangential points on each pulley and the synchronous belt. As shown in Figure 3, the driving, driven, and tension pulleys rotate by φ_1, φ_2, and φ_3, respectively. Inserting Eqs. (9) and (13) into Eq. (15), the pitch curves of driving pulley 1, driven pulley 2, and tension pulley 3 in fixed coordinate system $O_1 - XY$ are expressed as follows:

$$\begin{cases} X_1 = x_1\cos(\varphi_1) - y_1\sin(\varphi_1), \\ Y_1 = y_1\cos(\varphi_1) + x_1\sin(\varphi_1), \end{cases} \tag{17}$$

$$\begin{cases} X_2 = x_2\cos(\varphi_2) - y_2\sin(\varphi_2), \\ Y_2 = y_2\cos(\varphi_2) + x_2\sin(\varphi_2), \end{cases} \tag{18}$$

$$\begin{cases} X_3 = x_3\cos(\varphi_3) - y_3\sin(\varphi_3), \\ Y_3 = y_3\cos(\varphi_3) + x_3\sin(\varphi_3). \end{cases} \tag{19}$$

The coordinates of tangent points C_1, C_2, C_3, C_4, C_5 and C_6 in fixed coordinate system $O_1 - XY$ are X_{12} and Y_{12}, X_{21} and Y_{21}, X_{23} and Y_{23}, X_{34} and Y_{34}, X_{35} and Y_{35}, X_{16} and Y_{16}, respectively. The lengths of common tangent lines $\overline{C_1C_2}$, $\overline{C_3C_4}$, and $\overline{C_5C_6}$ between the driving and driven pulleys, driven and tension pulleys, and driving and tension pulleys are expressed as follows, respectively:

$$\begin{cases} \overline{C_1C_2} = \sqrt{(X_{12} - X_{21})^2 + (Y_{12} - Y_{21})^2} \\ \overline{C_3C_4} = \sqrt{(X_{23} - X_{34})^2 + (Y_{23} - Y_{34})^2} \\ \overline{C_5C_6} = \sqrt{(X_{35} - X_{16})^2 + (Y_{35} - Y_{16})^2} \end{cases}. \tag{20}$$

The tangential angles of tangent points C_6, C_2, C_3, C_4, C_5, and C_1 in moving coordinate systems $o_1 - x_1y_1$, $o_2 - x_2y_2$ and $o_3 - x_3y_3$ are θ_{12} and θ_{16}, θ_{21} and θ_{23}, θ_{34} and θ_{35}, respectively. The synchronous belt forms wrapping arc lengths with the driving, driven, and tension pulleys in areas C_2C_3, C_4C_5, and C_6C_1, respectively, which can be calculated as follows:

$$\begin{cases} \overset{\frown}{C_6C_1} = \int_{\theta_{16}}^{\theta_{12}} (p_1(\theta_1) + p_1''(\theta_1))\mathrm{d}\theta_1, \\ \overset{\frown}{C_2C_3} = \int_{\theta_{23}}^{\theta_{21}} (p_2(\theta_2) + p_2''(\theta_2))\mathrm{d}\theta_2, \\ \overset{\frown}{C_4C_5} = \int_{\theta_{35}}^{\theta_{34}} (p_3(\theta_3) + p_3''(\theta_3))\mathrm{d}\theta_3. \end{cases} \tag{21}$$

Substituting Eqs. (20) and (21) into Eq. (16), the belt length of the three-pulley noncircular synchronous belt transmission mechanism is expressed as follows:

$$\begin{aligned} S = & \sqrt{(X_{12} - X_{21})^2 + (Y_{12} - Y_{21})^2} \\ & + \sqrt{(X_{23} - X_{34})^2 + (Y_{23} - Y_{34})^2} \\ & + \sqrt{(X_{35} - X_{16})^2 + (Y_{35} - Y_{16})^2} \\ & + \int_{\theta_{16}}^{\theta_{12}} (p_1(\theta_1) + p_1''(\theta_1))\mathrm{d}\theta_1 \\ & + \int_{\theta_{23}}^{\theta_{21}} (p_2(\theta_2) + p_2''(\theta_2))\mathrm{d}\theta_2 \\ & + \int_{\theta_{35}}^{\theta_{34}} (p_3(\theta_3) + p_3''(\theta_3))\mathrm{d}\theta_3. \end{aligned} \tag{22}$$

3 Tension Pulley Pitch Curve Calculation of Three-Pulley Noncircular Synchronous Belt Drive with Minimum Slack

The circular–noncircular–noncircular three-pulley synchronous belt transmission mechanism comprises driving pulley 1 with a circular pitch curve, driven pulley 2 with a noncircular pitch curve, and tension pulley 3 with a noncircular pitch curve. The three pulleys had equal circumferences. The rotational relationship between the driving and driven pulleys is denoted as i_{12}, and the center distance of the three pulleys is $l_1 = l_2 = l_3$. An automatic optimization algorithm was developed, and the optimal solution was used to obtain the noncircular tension pulley pitch curve with the minimum slack.

3.1 Noncircular Belt Pulley Pitch Curve Concave and Convex Judgment Based on Vector Ipsilateral

As shown in Figure 5, n discrete points on the noncircular pulley pitch curve were used as n vertices of the constituent polygon, denoted counterclockwise as $P_i(i = 1, 2 \cdots, n)$. The coordinates of the vertices P_i were $(x_i, y_i)(i = 1, 2 \cdots, n)$. To determine the positional relationship between the edge of the polygon and the discrete point to be measured, i.e., to determine whether the discrete point to be measured is on the left or right of the edge (where the left and right sides are relative to the forward direction, which refers to the starting point to the end point of the line segment), one side of the polygon P_1P_2 was assigned to vector $\overrightarrow{P_1P_2}$, and the discrete point to be tested was P_3. Based mathematical geometry, the area of the triangle formed by three points P_1, P_2, and P_3 on the plane is expressed as follows [19]:

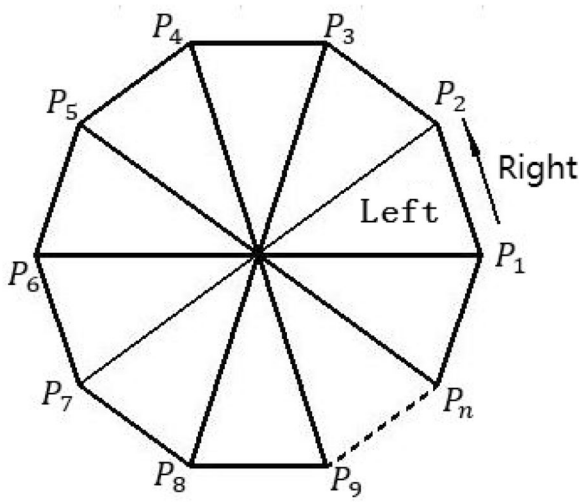

Figure 5 Assessment of positional relationship of discrete points of curved polygon

$$\begin{aligned} S(P_1, P_2, P_3) &= |y_1 \ y_2 \ y_3| \\ &= (x_1 - x_3)(y_2 - y_3) - (y_1 - y_3)(x_2 - x_3). \end{aligned} \tag{23}$$

If $S(P_1, P_2, P_3) > 0$, then P_3 is on the left side of the vector $\overrightarrow{P_1P_2}$. If $S(P_1, P_2, P_3) < 0$, then P_3 is on the right side of the vector $\overrightarrow{P_1P_2}$. If $S(P_1, P_2, P_3) = 0$, then P_3 is on line segment $\overrightarrow{P_1P_2}$. Similarly, if $S(P_1, P_2, P_3) > 0$ and $S(P_1, P_2, P_n) > 0$, then the polygon is convex at edge P_1P_2. Similarly, the positional relationship between each edge of the polygon and its two adjacent discrete points is calculated until all edges become convex [20, 21].

If it is determined that the polygon composed of discrete points is a convex polygon, then a convex noncircular pulley pitch curve can be obtained by fitting a cubic non-uniform B-spline [22, 23].

3.2 Three-Pulley Noncircular Synchronous Belt Slack Calculation Model

During one rotation period of the driving pulley, at some point j ($j = 1, 2, \ldots, n$), the circumference of the synchronous belt is S_j; $\max(S_j)$ and $\min(S_j)$ are the maximum and

minimum of the theoretical belt length in the next transmission cycle, respectively. The slack F is calculated as follows:

$$F = \max(S_j) - \min(S_j). \tag{24}$$

Figure 6 shows that the initial tension pulley pitch curve is the same as the driving pulley pitch curve, where the radius is R. Coordinate system $O_1 - X_1Y_1$ is established based on the initial tension pulley rotation center O_1. To ensure the accuracy of the tension pulley pitch curve and minimize the number of calculations, based on the principle of initial point selection of the optimization algorithm, points on the initial tension pulley pitch curve were obtained at every 45° and labeled as $A_i(i = 1, 2 \ldots, 8)$. $B_i(i = 1, 2 \ldots, 8)$ is the point on the extension line toward the diameter $\overrightarrow{O_1A_i}(1, 2, \ldots, 8)$. The length x_i (increment in radius) of vector $\overrightarrow{A_iB_i}$ was used as the design variable.

$$X = [x_1, x_2, x_3, x_4, x_5, x_6, x_7, x_8]. \tag{25}$$

To minimize the belt slack of the noncircular three-pulley synchronous belt drive mechanism, the minimum value of the belt slack was obtained directly as the objective function [24, 25]:

$$\min F(x) = \max(S(i)) - \min(S(i)), \quad i = 1,\ 2,\ 3, \ldots,\ 720. \tag{26}$$

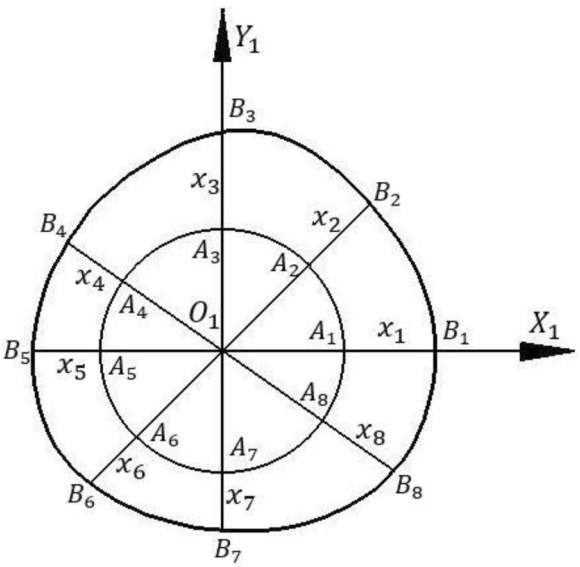

Figure 6 Selection of design variables for automatic optimization algorithm

3.3 Optimal Calculation of Tensioned Pulley Pitch Curve with Minimum Slack

As shown in Figure 7, to ensure that the algorithm can quickly search for the optimal solution within the optimization region, the value range of the design variable (the optimization region) must be selected, where $X(i)_{\max}$ and $X(i)_{\min}$ are the upper and lower limits of the ith variable, respectively. $D(i) = X(i)_{\max} - X(i)_{\min}$ is the allowable change in diameter. The selection of the upper and lower limits of the design variables should be considered comprehensively based on the objective function, design requirements, and algorithm execution time. The expression for the range of the design variables is as follows:

$$X(i)_{\min} \le X(i) \le X(i)_{\max}\ ,\ \ i = 1, 2, \ldots, 8. \tag{27}$$

To ensure that the noncircular tension pulley pitch curve is convex, i.e., to ensure that the polygon composed of discrete points $B_i(i = 1,\ 2, \ldots,\ 8)$ on the noncircular tension pulley is convex, the radius of the circular pitch curve of the initial tension pulley is R, the coordinates of $B_i(i = 1, 2, \ldots, 8)$ are (M_i, N_i), the abscissa $M_i = (R + x_i)\cos(\pi i/4)$, the ordinate $N_i = (R + x_i)\sin(\pi i/4)$, and the constraint equations are as follows [26]:

$$\begin{cases} (M_1 - M_3)(N_2 - N_3) - (N_1 - N_3)(M_2 - M_3) > 0, \\ (M_2 - M_4)(N_3 - N_4) - (N_2 - N_4)(M_3 - M_4) > 0, \\ (M_3 - M_5)(N_4 - N_5) - (N_3 - N_5)(M_4 - M_5) > 0, \\ (M_4 - M_6)(N_5 - N_6) - (N_4 - N_6)(M_5 - M_6) > 0, \\ (M_5 - M_7)(N_6 - N_7) - (N_5 - N_7)(M_6 - M_7) > 0, \\ (M_6 - M_8)(N_7 - N_8) - (N_6 - N_8)(M_7 - M_8) > 0, \\ (M_7 - M_1)(N_8 - N_1) - (N_7 - N_1)(M_8 - M_1) > 0, \\ (M_8 - M_2)(N_1 - N_2) - (N_8 - N_2)(M_1 - M_2) > 0. \end{cases} \tag{28}$$

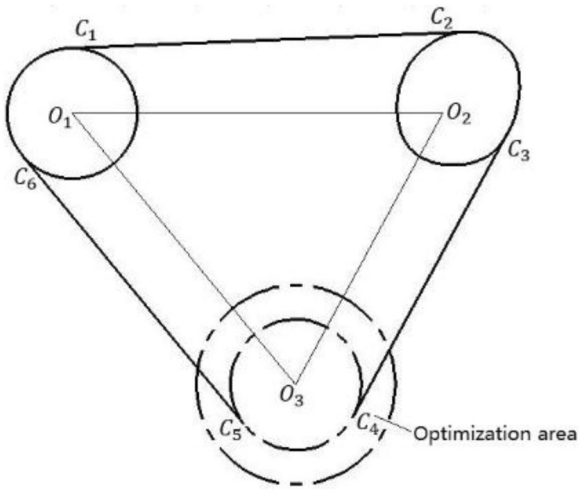

Figure 7 Schematic of search area of automatic search algorithm

One rotation cycle of the driving pulley in the noncircular synchronous belt drive mechanism is considered as one cycle segmented into 720 moments at the *j*th time. The belt length of the three-pulley noncircular synchronous belt transmission mechanism is $S(j)$ [27]. The minimum ($\Delta S_{\min}$) value of the difference between the maximum ($S_{\max}$) pulley length and minimum pulley length ($S_{\min}$) in a period is used as a fitness function, as follows:

$$\begin{cases} S_{\max} = \max(S(j)), \ (j = 1, 2, 3, \ldots, 720), \\ S_{\min} = \min(S(j)), \ (j = 1, 2, 3, \ldots, 720), \\ \Delta S_{\min} = S_{\max} - S_{\min}. \end{cases} \tag{29}$$

Based on the objective function and constraint conditions, 720 points around the tension pulley were considered as the optimized individual group. Every 45° point on the circumference of a non-circle was selected, and eight points were used as optimization points. An adaptive evolutionary algorithm was designed to iteratively optimize the initial tension pulley based on the minimum synchronous belt slack. The largest number of iterations was 100, and the convergence criterion was a change of less than 1×10^{-4} in the objective function. The optimized point was interpolated using a B-spline function to fit the curve of the noncircular tension pulley. The algorithm flowchart is shown in Figure 8, and the optimization solution was obtained.

3.4 Transmission Characteristics Analysis Software for Three-pulley Noncircular Synchronous Belt with Minimum Slack

As shown in Figure 9, Region 1 is the parameter input area. The basic parameters of the noncircular three-pulley synchronous belt transmission mechanism were input to the fields in this region. The main parameters of the noncircular three-pulley synchronous belt transmission mechanism included the three belt pulley rotation center coordinates, driving pulley radius, driving and driven pulley transmission ratios, maximum allowable synchronous belt slacks, and initial radius of the tension pulley [28, 29]. Region 2 is the basic control and optimization control area, which included three basic control buttons for the starting, ending, and equal perimeter calculations as well as two optimization control buttons for tension pulley fitting and automatic optimization. The display area of the basic parameters was used to display the center distance, real-time belt length, and slacks of two adjacent pulleys during the simulation of the noncircular three-pulley synchronous belt transmission mechanism. Region 4 is the pitch curve display area, which was used to display the optimal pitch curve of the tension pulley obtained after an automatic optimization, and the noncircular pitch curve of the tension pulley was calculated using an equal circumference. Region 5 is the motion simulation area, which was used to display the real-time

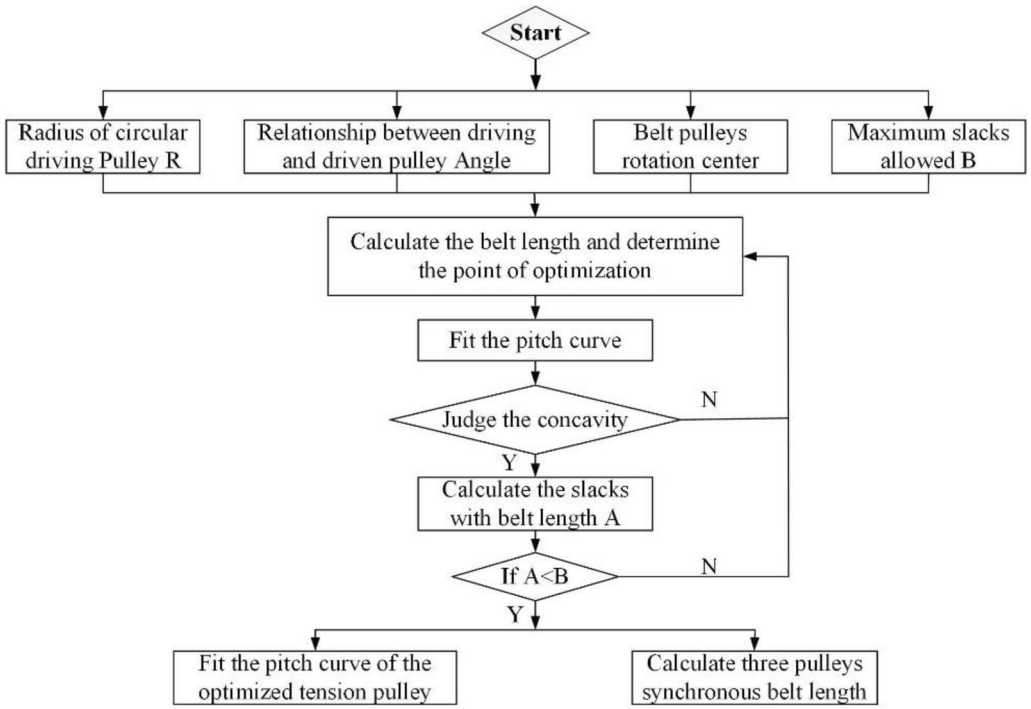

Figure 8 Flow chart of automatic optimization algorithm

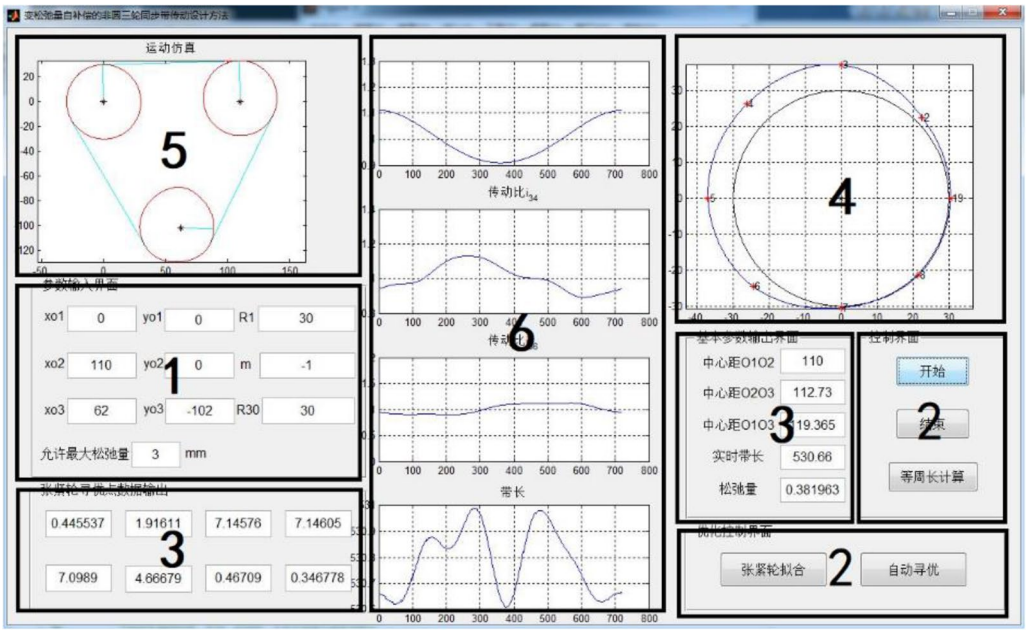

Figure 9 Noncircular three-pulley synchronous belt transmission optimization design software

motion simulation process of the noncircular three-pulley synchronous belt transmission mechanism. Region 6 is the calculation result area, which was used to display the calculation results of the noncircular three-pulley synchronous belt drive mechanism, including the transmission ratio between two adjacent pulleys and the belt length variation curve.

3.5 Comparison and Analysis of Noncircular Three-Pulley Synchronous Belt Drive with Minimum Slack

3.5.1 Analysis of Minimum Slack in Eccentric Circular Three-Pulley Synchronous Belt Transmission Mechanism

Because the pitch curve of the driving pulley was circular, the coordinates of rotation center o_1 were $xo_1 = 0$ and $yo_1 = 0$. The radius of the driving pulley was $R_1 = 30$. The curve of the driven pulley was an eccentric circle, and the coordinates of rotation center o_2 were $xo_2 = 110$ and $yo_2 = 0$. The eccentricity $e_2 = 15$ and $R_2 = 30$. The rotation center coordinates of the tension pulley were $xo_3 = 62$ and $yo_3 = -102$. The mechanism was a circular eccentric–noncircular three-pulley synchronous belt transmission mechanism. A method reported previously [7] was adopted for manual optimization. The belt length change curve obtained is shown in Figure 10; its slack was approximately 10.36 mm. However, the automatic optimization algorithm presented above was adopted for optimization and adjustments. The variation curve of the band length is shown in Figure 11; its slack was 0.03 mm. The pitch curves of the tension pulley before and after optimization are shown in Figure 12; it is clear that the automatic optimization algorithm used in this study was high in accuracy [30].

3.5.2 Analysis of Minimum Slack under Different Transmission Ratio Laws

Because the pitch curve of the driving pulley was circular, the coordinates of rotating center o_1 were $xo_1 = 0$ and yo_1

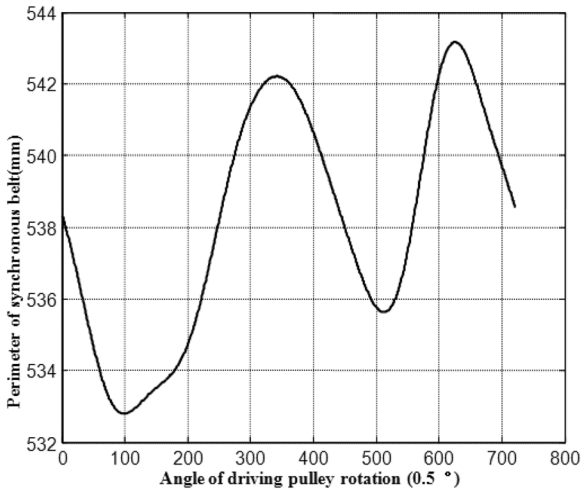

Figure 10 Belt length variation curve after manual optimization of tension pulley pitch curve

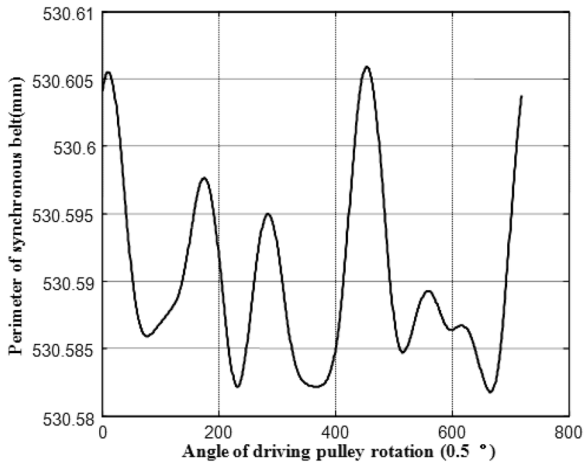

Figure 11 Belt length variation curve after automatic optimization of tension pulley pitch curve

$= 0$. The radius of the driving pulley, $R_1 = 30$. The pitch curve of the driven pulley was noncircular, and the coordinates of the rotating center o_2 were xo_2=110 and yo_2=0. The eccentricity e_2=15 and R_2=30. The rotation center coordinates of the tension pulley were $xo_3 = 62$ and $yo_3 = -102$. The driving and driven pulleys were rotated by angles φ_1 and $\varphi_2 = \varphi_1 + m \cdot \sin(\varphi_1)$, respectively, where m was set as different values to verify the rationality and validity of the automatic optimization algorithm. The other parameters of the noncircular three-pulley synchronous belt transmission mechanism were the same. For $m = -0.2$, -0.1, 0.1, and 0.2, the belt length variation and tension pulley pitch curves are as shown in Figures 12 and 13, respectively. The corresponding slacks were 0.858, 0.379, 0.166, and 0.725 mm, respectively. By setting different m values, i.e., for different transmission ratios, the automatic optimization algorithm can solve for the discrete data points on the optimal noncircular tension pulley pitch curve; subsequently, the latter can be obtained by non-uniform rational B-splines fitting.

The specific parameters of the automatic optimization algorithm were compared for different transmission ratios, as shown in Table 1. Table 1 and Figures 13 and 14 show that when other conditions remained unchanged, the execution time and slacks of the automatic optimization algorithm differed for different transmission ratios (different values of m). The "zigzag" fluctuations of the transmission ratio curve were related to the number of data points on the pitch curve and the accuracy in the tangent calculation method. Specifically, the closer m is to 0 (the driven pulley closer to the circle), the smaller is the slack, as calculated by the allowable variation in the same directional diameter, and the shorter is the execution time of the corresponding algorithm. In general, the automatic optimization algorithm converged, and the convergence speed was faster.

3.5.3 Analysis of Minimum Slack Amount under Different Radial Diameter Allowable Changes

To study the effect of the directional diameter (i.e., D values) on the automatic optimization algorithm, for $m = -0.1$, D was assigned the values shown in Table 2 and substituted into the algorithm. The belt length variation curve obtained after the operation is shown in Figure 15. As shown in Table 2, the allowable variation in the directional diameter D significantly affected the slack and execution time of the algorithm after automatic optimization. In particular, the larger the range of the absolute

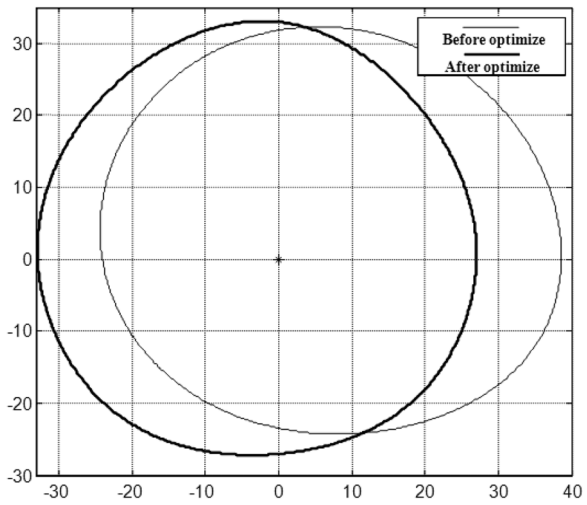

Figure 12 Tension pulley joint curve before and after optimization

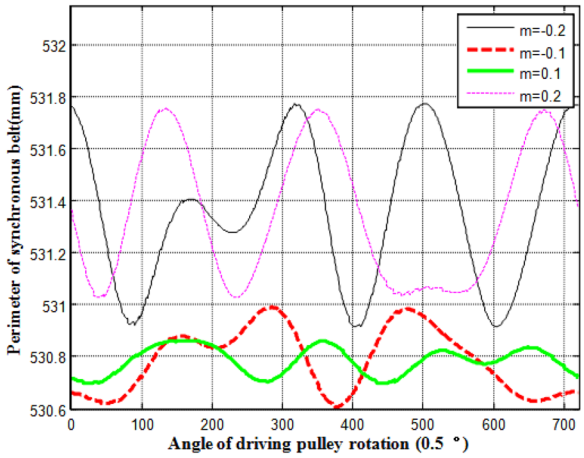

Figure 13 Variation curve of belt length for different transmission ratios

Table 1 Comparison of related objects of automatic optimization algorithm under different transmission ratio laws

Object	$m = -0.2$	$m = -0.1$	$m = 0.1$	$m = 0.2$
Slack (mm)	0.858	0.379	0.166	0.725
Algorithm execution time (s)	66862	54441	54186	70817
Iterative convergence of algorithm	Converged	Converged	Converged	Converged

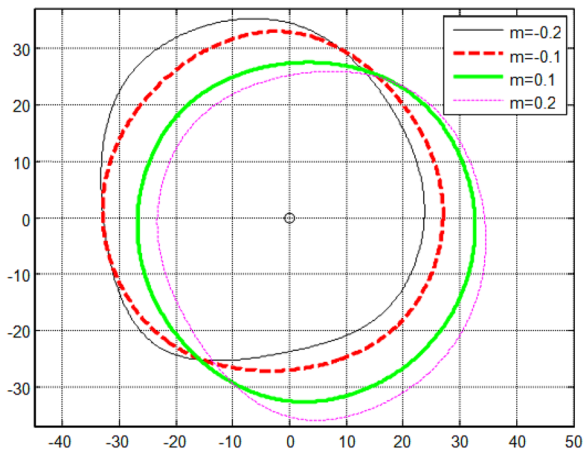

Figure 14 Tension pulley pitch curve corresponding to different *m* values

value of variable *D*, the larger was the optimization area that allowed for the maximum slack $\Delta L_{\max}$, which reduced the possibility of obtaining an optimal solution. Furthermore, the possibility of obtaining an exact solution containing a smaller slack became greater, and the smaller the slack, the longer was the execution time of the algorithm. As shown in Figure 14, for different diameter values *D*, the automatic optimization algorithm converged quickly and obtained discrete data points on the optimal noncircular tension pulley pitch curve.

In summary, it is critical to set a reasonable *D* value for a noncircular three-pulley synchronous belt transmission mechanism using an automatic optimization algorithm to calculate the optimal noncircular tension pulley.

4 Experimental Research on Three-Pulley Noncircular Synchronous Belt Transmission

4.1 Development of Testbed

The coordinates of the rotation center O_1 of the driving pulley of the testbed were $xo_1 = 0$ and $yo_1 = 0$, and the radius of the driving pulley was $R_1 = 30$. The coordinates of the rotation center O_2 of the driven pulley were $xo_2 = 110$ and $yo_2 = 0$. The central coordinates of the tension pulley were $xo_3 = 62$ and $yo_3 = -102$, and the rotation angle of the driven pulley was $\varphi_2 = \varphi_1 - 0.1 \times \sin(\varphi_1)$. The testbed primarily included a transmission mechanism, testbed frame, driving motor, counting equipment, and tension control equipment, as shown in Figure 16.

A direct current motor deceleration motor was connected to the circular driving pulley (the original part) through plum blossom coupling and rotated at a uniform speed, followed by a noncircular driven pulley and

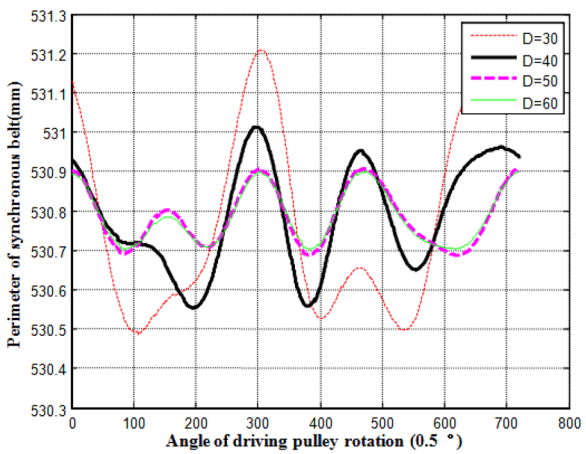

Figure 15 Band length variation curve corresponding to different directional diameters D

Table 2 Comparison of related objects of automatic optimization algorithm under different absolute range values of variables

Object	$D = 30$	$D = 40$	$D = 50$	$D = 60$
Slack (mm)	0.693	0.437	0.219	0.195
Algorithm running time (s)	39333	46258	53936	62398
Iterative convergence of algorithm	Converged	Converged	Converged	Converged

a tension pulley. The other end of the three synchronous pulleys was connected to the encoder, and the encoder was fixed on the testbed frame, which was used to measure the rotational speed of the three synchronous pulleys to obtain the actual transmission ratio of the experiment. The DC deceleration motor was connected to the speed regulation module to adjust the speed of the motor output shaft. To analyze the effect of the load torque on the transmission period of the noncircular three-pulley synchronous belt drive mechanism, a micro magnetic powder brake was installed on the driven pulley shaft, and the load torque loaded on the driven pulley through the current was adjusted by the tension controller.

4.2 Test Results and Analysis

A load torque was applied to the driven wheel shaft through a magnetic powder brake. The rotational speeds of encoders A and B were obtained using an IPAM7404, and the data were transmitted to a computer through an RS485 converter. The fitting curve was compared to the theoretical curve by fitting the test discrete data points in MATLAB.

Figure 17 shows the discrete data point fitting results of the transmission ratio of the driving pulley to the driven pulley, and Figure 18 shows a comparison of the fitted and theoretical curves of the transmission ratio of the driving pulley to the driven pulley. As shown in Figure 17, the discrete data points of the test transmission ratio generally exhibited a regular trend and fluctuated within the minimum error range, and the data exhibited statistical significance. A smooth transmission ratio fitting curve was obtained using MATLAB. As shown in Figure 18, the trend of the actual transmission ratio curve fitted by the test discrete point data was similar to the theoretical transmission ratio curve. The transmission characteristics of a three-pulley noncircular synchronous belt transmission mechanism with a minimum amount of slack in the synchronous belt were verified in this study. The change in the transmission ratio obtained from the test was consistent with the theoretical value; therefore, an accurate non-uniform speed and a significant center distance transmission can be achieved.

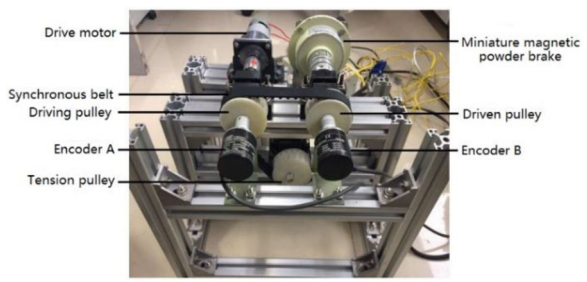

Figure 16 Front view of noncircular three-pulley synchronous belt transmission mechanism test rig

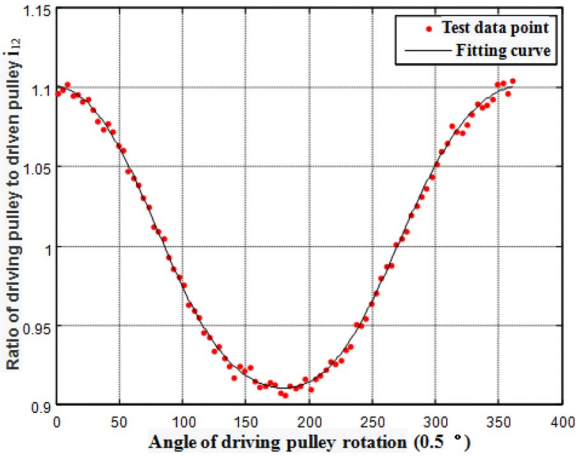

Figure 17 Simulation results of master–slave transmission ratio

5 Conclusions

(1) In this study, a model for calculating the slack of a three-pulley noncircular synchronous belt transmission mechanism was developed, and an optimal calculation method for the noncircular tensioned pulley pitch curve of a three-pulley noncircular synchronous belt transmission mechanism with minimum slack was proposed.

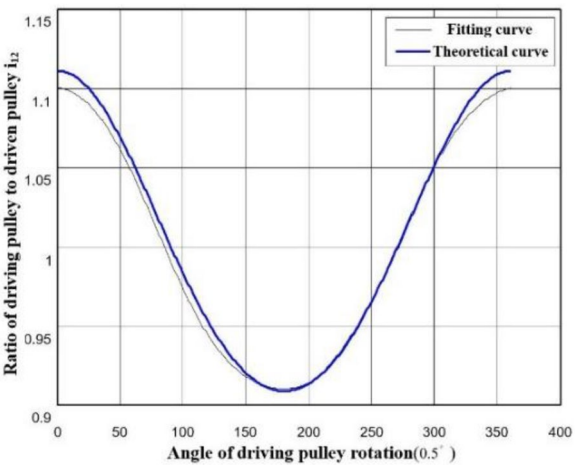

Figure 18 Comparison of analogy results of master–slave drive

(2) Based on the calculation and optimization models of the three-pulley noncircular synchronous belt transmission mechanism, the motion simulation, analysis, and optimization code of the transmission mechanism was written, and the characteristics of the minimum slack of different non-uniform transmission ratio laws were analyzed based on multiple examples.

(3) A circular–noncircular–noncircular synchronous belt pulley transmission mechanism test rig was developed, and experimental research was conducted. It was discovered that the output characteristics of the driven pulley were consistent with the theoretical characteristics. The reliability of the analytical calculation and optimization models of the three-pulley noncircular synchronous belt transmission mechanism was verified.

Acknowledgements
Not applicable.

Authors' Information
Jianneng Chen, born in 1972, is currently a professor at *Zhejiang Sci-Tech University, China*. He received his PhD degree from *Zhejiang University, China*, in 2004. His research interests include mechanism analysis and synthesis, agricultural machinery equipment, and technology.

Xincheng Sun, born in 1979, is currently a PhD candidate at *Zhejiang Sci-Tech University, China*. He received his bachelor's degree from *Northwest A&F University, China*, in 2007. His research interests include mechanism design and agricultural planting equipment.

Chuanyu Wu, born in 1976, is currently a professor at *Zhejiang Sci-Tech University, China*. His research interests include theory and application of mechanism innovative design, robot technology, and application.

Dadu Xiao, born in 1993, is currently an engineer at *Zhejiang Dahua Technology Co., Ltd., China*.

Jun Ye, born in 1989, is currently a PhD candidate at *Zhejiang Sci-Tech University, China*. His research interests include mechanism design and robotics.

Authors' contributions
XS was responsible for the entire trial; XS wrote the manuscript; XS, JC, CW, DX, and JY assisted with experiments and data analysis. All authors read and approved the final manuscript.

Funding
Supported by National Natural Science Foundation of China (Grant Nos. 51675486, 51805487).

Competing interests
The authors declare no competing financial interests.

Author Details
[1] Faculty of Mechanical Engineering and Automation, Zhejiang Sci-Tech University, Hangzhou 310018, China. [2] Zhejiang Key Laboratory of Planting Equipment Technology, Hangzhou 310018, China.

Received: 10 February 2020 Revised: 4 December 2020 Accepted: 19 February 2021
Published online: 06 March 2021

References

[1] H Satchel. Non-uniform chain-wheel drives. 8thWorld Congress on TMM, Pragal, Czechoslovakia, 1991.
[2] Xutang Wu, Guihai Wang. *Noncircular gear and non-uniform ratio transmission*. Beijing: China Machine Press, 1997. (in Chinese)
[3] Xutang Wu. Calculation principle of joint curve of noncircular sprocket (belt pulley). *Mechanical Transmission*, 1993, 17(2): 13-17.
[4] I Yamakage, T Konishi, M Horio, et al. Studies and development of a high performance rice transplanter. *J. Jpn. Soc. Agric. Mach.*, 1989, 51(6): 604-610.
[5] L S Guo, W J Zhang. Kinematic analysis of a rice transplanting mechanism with eccentric planetary gear trains. *Mech. Mach. Theory*, 2001, 36(11): 1175-1188.
[6] D Liu, T Ren. Study on deformed limacon gear and motion iterative of its serial mechanism. *J. Mech. Des.*, 2011, 133(6): 061004.
[7] E Ottaviano, D Mundo, G A Danieli, et al. Numerical and experimental analysis of noncircular gears and cam-follower systems as function generators. *Mech. Mach. Theory*, 2008, 43(8): 996-1008.
[8] F S Li. *Noncircular gear*. Beijing: Mechanical Industry Press, 1975. (in Chinese)
[9] O Karpov, P Nosko, P Fil, et al. Prevention of resonance oscillations in gear mechanisms using noncircular gears. *Mech. Mach. Theory*, 2017, 114: 1-10.
[10] F Freudenstein, C K Chen. Variable-ratio chain drives with noncircular sprockets and minimum slack-theory and application. *Journal of Mechanical Design*, 1991, 113(3): 253-262.
[11] Enlai Zheng, Fang Jia, Hongwei Sha, et al. Noncircular belt transmission design of mechanical press. *Mechanism and Machine Theory*, 2012, 57(11): 126-138.
[12] Liping Feng, Jiahong Zheng. Optimization of noncircular sprocket drive segment curve. *Mechanical Design*, 2006, 23(1): 25-27.
[13] Yuping Yang, Binbin Ji. Optimal design of tensioning wheel installation position in synchronous belt transmission. *Journal of Nantong University*, 2010, 9(1): 68-70.
[14] Lixin Cao, Jian Liu. Research on the mapping models and designing methods of variable-ratio chain/belt drives. *Mechanism and Machine Theory*, 2002, 37: 955-970.
[15] Xiaojing He. *Research on design method and key technology of three-pulley noncircular synchronous belt transmission*. Hangzhou: Zhejiang University of Science and Technology, 2017.
[16] Xutang Wu. Contour design of noncircular steel belt transmission. *Mechanical Design*, 1999(11): 10-12.
[17] Wei Wang, Chen Zhao. Proof of calculation formula of radial, vector and tangent positive angle of plane curve. *Journal of Tianjin Normal University (Nature Edition)*, 1999, 19(3): 67–70.
[18] Kai Yu. Algorithm of distinguishing inner and outer points of convex polygon based on dichotomy. *Electronic Design Engineering*, 2016, 24(16): 187-190.
[19] Yajun Yang, Mingyi Duan. An improved algorithm for determining the relationship between a point and a specified polygon region. *Computer Knowledge and Technology*, 2014, 10(22): 5362-5364.
[20] Xiaoxiang Zhao. Using iteration method to find common tangent. Science and Education Guide, 2015(13): 28-32.
[21] M Masal, M Tosun, A Z Pirdal. Euler savary formula for the one parameter motions in the complex plane C. *Int. J. Phys. Sci.*, 2010, 5(1): 6-10.

[22] N R Miller, D Ross. Design of variable-ratio chain drives for bicycles and ergometers-application to a maximum power bicycle drive. *J. Mech. Des.*, 1980, 102(4): 711-717.
[23] L A Piegl, W Tiller. Fitting NURBS spherical patches to measured data. *Eng. Comput.*, 2008, 24(2): 97-106.
[24] M F Tsay, Z H Fong. Study on the generalized mathematical model of noncircular gears. *Math. Comput. Model*, 2005, 41(4): 555-569.
[25] Y M Zhang, Q Liu, B Wen. Practical reliability-based design of gear pairs. *Mech. Mach. Theory*, 2003, 38(12): 1363-1370.
[26] X Liu, A Fahad, Y Kazuo, et al. Adaptive interpolation scheme for NURBS curves with the integration of machining dynamics. *Int. J. Mach. Tools Manuf.*, 2005, 45(4): 433-444.
[27] H X Ju. Design and kinematics analysis of noncircular belt drive. *J. Mech. Transm.*, 2015, 39(1): 126-130.
[28] F Zheng, L Hua, X Han, et al. Generation of noncircular bevel gears with free-form tooth profile and tooth tengthwise based on screw theory. *J. Mech. Des.*, 2016, 138(6): 064501.
[29] F Y Zheng, H Lin, X H Han, et al. Synthesis of indexing mechanisms with noncircular gears. *Mech. Mach. Theory*, 2016, 105: 108-128.
[30] Carlo Innocenti, Davide Paganelli. Designing synchronous belt transmissions with variable velocity ratio. *Journal of Mechanical Design*, 2008, 130(1): 842-849.